Translating *in vivo* metabolomic analysis of succinate dehydrogenase deficient tumours into clinical utility

Ruth T Casey[1, 2], Mary A McLean[3], Basetti Madhu[3], Benjamin. G Challis[2], Rogier. ten Hoopen[4], Thomas. Roberts[5], Graeme. R. Clark[1], Deborah Pittfield[2], Helen L Simpson[6], Venkata R Bulusu[7], Kieran Allinson[8], Lisa Happerfield[9], Soo-Mi Park[1], Alison Marker[8], Olivier Giger[4], Eamonn R Maher [*1], Ferdia A Gallagher[*3, 10].

1. Department of Medical Genetics, University of Cambridge and NIHR Cambridge Biomedical Research Centre and Cancer Research UK Cambridge Centre, CB2 OQQ, United Kingdom.

2. Department of Endocrinology, Cambridge University NHS Foundation Trust, Cambridge, CB2 OQQ, United Kingdom.

3. Cancer Research UK Cambridge Institute, University of Cambridge, Li Ka Shing Centre, Robinson Way, Cambridge CB2 0RE, UK

4. Department of Pathology, University of Cambridge, Addenbrooke's Hospital, Cambridge, CB2 0QQ, UK.

5. Haematology Oncology Diagnostic Service (HODS), Cambridge University NHS Foundation Trust, Cambridge, CB2 OQQ, United Kingdom.

6. Department of Diabetes and Endocrinology, University College London Hospitals, NHS Foundation Trust, London, NW1 2PG UK

7. Department of Medical Oncology, Cambridge University NHS Foundation Trust, Cambridge, CB2 OQQ, United Kingdom.

8. Department of Histopathology Cambridge University NHS Foundation Trust and Cancer Research UK Cambridge Centre Cambridge, CB2 0QQ, United Kingdom.

9. Department of Immunohistochemistry, Cambridge University NHS Foundation Trust, Cambridge, CB2 OQQ, United Kingdom.

10. Department of Radiology, Cambridge University NHS Foundation Trust, CB2 OQQ, United Kingdom.

***= joint last author**

Corresponding author: Dr Ruth Casey, Department of Medical Genetics, University of Cambridge and NIHR Cambridge Biomedical Research Centre and Cancer Research UK Cambridge Centre, CB2 OQQ, United Kingdom.

Mobile: 07401 179473, Email: rc674@medschl.cam.ac.uk

Running title: *In vivo* metabolomic analysis of succinate dehydrogenase deficient tumours

Key words: Translational, metabolic cancer, metabolomics, hereditary, imaging technique

Word count: 3000

References: 30

Figures: 5

Tables 1

Supplementary figures: 1

Supplementary tables: 2

The authors have nothing to declare and there are no conflict of interests to report.

Disclosure: The authors have declared no conflicts of interest.

To date this research was presented as an abstract at the European Congress of Endocrinology in Lisbon in May 2017.

Abstract

Purpose: Mutations in the mitochondrial enzyme succinate dehydrogenase (SDH) subunit genes are associated with a wide spectrum of tumours including phaeochromocytoma and paraganglioma (PPGL) [1, 2], gastrointestinal stromal tumours (GIST) [3], renal cell carcinoma (RCC) [4] and pituitary adenomas[5]. SDH-related tumorigenesis is believed to be secondary to accumulation of the oncometabolite succinate. Our aim was to investigate the potential clinical applications of MRI spectroscopy (^{1}H-MRS) in a range of suspected SDH-related tumours.

Patients and methods: Fifteen patients were recruited to this study. Respiratory-gated single-voxel ^{1}H-MRS was performed at 3T to quantify the content of succinate at 2.4 ppm and choline at 3.22 ppm.

Results: A succinate peak was seen in six patients, all of whom had a germline *SDHx* mutation or loss of SDHB by immunohistochemistry. A succinate peak was also detected in two patients with a metastatic wild-type GIST (wtGIST) and no detectable germline *SDHx* mutation but a somatic epimutation in *SDHC*. Three patients without a tumour succinate peak retained SDHB expression, consistent with SDH functionality. In six cases with a borderline or absent peak, technical difficulties such as motion artefact rendered ^{1}H-MRS difficult to interpret. Sequential imaging in a patient with a metastatic abdominal paraganglioma demonstrated loss of the succinate peak after four cycles of [^{177}Lu]-DOTATATE, with a corresponding biochemical response in normetanephrine.

Conclusions: This study has demonstrated the translation into clinical practice of *in vivo* metabolomic analysis using ^{1}H-MRS in patients with SDH-deficient tumours. Potential applications include non-invasive diagnosis and disease stratification, as well as monitoring of tumour response to targeted treatments.

Introduction

The succinate dehydrogenase (SDH) enzyme is composed of four subunits (A-D) and has a key role in the Krebs cycle and oxidative phosphorylation[6]. In the past two decades germline mutations in the genes encoding the four SDH subunits (*SDHA*/*SDHB*/*SDHC*/*SDHD*), collectively known as *SDHx* have emerged as an important cause of human neoplasia and a paradigm for the role of disordered cellular metabolism in oncogenesis [1-5, 7]. *SDHx* mutations were described initially in association with head and neck paragangliomas (derived from parasympathetic ganglia) and in phaeochromocytomas and paragangliomas (PPGL, derived from sympathetic ganglia and often secreting catecholamines) [1, 2]. It is now recognised that approximately 40% of PPGL patients harbour a germline mutation in an inherited PPGL gene and *SDHx* mutations are the most common cause of PPGL predisposition[9]. In addition, germline *SDHB* mutations are associated with a high risk of malignancy in PPGL[9]. Other tumour types associated with *SDHx* mutations include gastrointestinal stromal tumours (GISTs) and renal cell carcinomas (RCCs)[10-13]. GISTs are mesenchymal tumours of the gastrointestinal tract and in adults usually associated with somatic activating mutations in the *KIT* or *PDGFRA* genes[3, 11]. However GISTs without *KIT* and *PDGFRA* gene mutations[3], known as wild-type (wtGIST), account for 15% of adult and 85% of paediatric GIST tumours and recent studies suggest that up to 88% of wtGIST are SDH-deficient[11]. wtGIST with SDH-deficiency may harbour a germline *SDHx* mutation (75% of cases) or an *SDHC* gene epimutation with hypermethylation of the promoter region[11]. Only about a third of patients with SDH-deficient wtGIST achieve disease stabilisation with imatinib therapy[12] and the risk of metastatic disease is higher for SDH-deficient GIST compared to conventional GIST[11, 12]. *SDHx*-associated RCC may present in patients with a personal or family history of PPGL or may present with an RCC-only phenotype[13]. Finally germline *SDHx* mutations have been described in rare patients with pituitary adenomas[10]. Despite recent advances in the

understanding of the *SDHx* genes, there are many areas of unmet clinical need including a lack of robust biomarkers to predict aggressive biological behaviour and to inform on clinical surveillance and management[14].

Succinate has been shown to be elevated by 100-fold in *SDHx*-mutated PPGL tumours *ex-vivo* compared with non-*SDHx* mutated PPGL tumours[15]. Recently, *in vivo* detection of succinate by MR spectroscopy was reported in two patient cohorts with SDH deficient PPGL[16, 17]. Similarly, the non-invasive detection of 2-hydroxyglutarate with ^{1}H-MRS has been demonstrated in glioma in patients with a gain of function mutation in another citric acid cycle enzyme, isocitrate dehydrogenase 1 (IDH1)[18]. The ability to measure succinate *in vivo* has a number of important potential clinical applications including early identification of SDH deficiency, which can enable tailored patient surveillance and management. *In vivo* detection of succinate accumulation could also serve to verify genetic variant pathogenicity in the era of next generation sequencing. The aim of this study was to investigate the role of ^{1}H-MRS in detecting abnormally elevated succinate *in vivo* in patients with suspected SDH deficient tumours, expanding the applications of ^{1}H-MRS in SDH deficient tumorigenesis to include GIST and pituitary adenoma for the first time and to explore the technique as a potential non-invasive biomarker of treatment response.

Methods

Patient selection

This study was performed as a prospective case series and subjects were recruited from a dedicated neuroendocrine tumour clinic and a national paediatric and adult wild-type (PAWS) GIST clinic in Cambridge University NHS Foundation Trust. Suitable patients were identified based on *SDHx* germline status, suspicious clinical phenotype (metastatic PPGL,

paraganglioma or wtGIST) and/or immunohistochemistry of tumour tissue showing absent SDHB immunostaining. A minimum tumour size threshold of 1.5cm was applied for inclusion into the study. All participants gave written informed consent and the study was approved by Cambridge South Research Ethics Committee.

MRS Analysis

Both SAGE (GE Healthcare, Waukesha, WI) and LCModel[19] spectroscopy analysis programmes were used to reconstruct, analyze and display spectra. For each metabolite, LCModel reports both peak area and the estimated uncertainty in fitting of the peak (%SD). This uncertainty measure was used to stratify the results using the following algorithm: 1) if %SD of choline was >15%, the spectrum was discarded as a technical failure, because it was assumed that choline should be detectable in a metabolically active tumour, such that SD>15% would indicate probable data quality issues; 2) succinate detection was taken as positive if its %SD was <50%, and negative if it was >50%. The succinate to choline ratio was quantified (SCR), the full width at half maximum height (FWHM) of the water peak in Hz was measured in SAGE and recorded as an additional data quality metric, and an expert spectroscopist was asked to rate whether detected succinate peaks were convincing or unconvincing based on data displayed both in LCModel and in SAGE.

Statistical methods, ^{1}H-MRS data acquisition, Germline genetic analysis, SDHB Immunohistochemistry, SDHC hypermethylation analysis and measurement of succinate in ex vivo tissue samples

See supplementary data.

Results

Patients and clinical phenotype

Fifteen subjects (6 females, 9 males; mean age 40 years (range 21-80 years) were studied. Seven wtGIST, three unilateral adrenal phaeochromocytomas, three abdominal PGL's, a large left glomus PGL and a non-functioning pituitary macroadenoma were examined. Nine patients (60%) had metastatic disease: six with wtGIST, two with an abdominal paraganglioma and one with a unilateral phaeochromocytoma. The liver was the most common site for metastases (7/9, 77.7%). Three patients had multicentric primary tumours, including subject #5 who presented with a metastatic wtGIST and was subsequently diagnosed with a 1.9 cm carotid body PGL (figure 2d, case 5), subject #9 with an abdominal paraganglioma and a small left sided 1.5 cm carotid paraganglioma (figure 3b, case 9), and subject #8 with a large left sided glomus paraganglioma and a 2 cm prolactin secreting pituitary adenoma (figure S1, case 8). Only two patients had a positive family history, (Table 1: case 2 and case 6).

Genotype

A germline mutation in a *SDHx* gene was identified in 9/15 (60%) of subjects: 5 in *SDHB* (4 missense variants and 1 truncating variant) and 4 in *SDHA* (1 missense and 3 truncating). Two further patients were diagnosed with a somatic *SDHC* epimutation (Table 1).

^{1}H-MRS succinate analysis

The ^{1}H-MRS characteristics of the 15 patients are shown in Supplementary Table S1. The mean size of the tumour selected for spectra acquisition was 5.5 cm (median: 3.3 cm, range: 1.8-12 cm). The liver was the most common site to be assessed (n = 6), but good quality

spectra were also obtained from the pituitary (n = 1), and PPGL tumours (n = 5). The subjects were divided into four groups according to whether a succinate tumour peak was: present, absent, a borderline peak was detected, or technical failure prevented interpretation of the spectra.

Succinate peak detected

Succinate was detected at 2.4 ppm in 6 patients (50 %). The mean SCR in these patients was 1.3 (SD ± 0.71) and the mean tumour size in those six patients with reliable succinate peak detection was 4.8 cm (SD ± 2.94, range 2.3-9 cm). The *in vivo* detection of succinate on ^{1}H-MRS correlated with tumour SDH deficiency: 4 of the 6 cases had a germline *SDHx* mutation and loss of SDHB expression on immunohistochemistry and a somatic *SDHC* epimutation was detected in 2 of the 6 (Figure 1).

Borderline succinate peak detected

A borderline succinate peak was detected in two subjects. Patient #8 with a germline *SDHB* mutation (c.600G>T p.Trp200Cys) and a glomus paraganglioma, demonstrated an SCR of 1.19; however the linewidth (29 Hz) was so broad due to the proximity of metallic dental work that the peak assignments were not reliable (Figure S1). Patient #7 with a metastatic phaeochromocytoma and no detectable germline *SDHx* mutation demonstrated an SCR of 0.18 but the LCModel detected a very small succinate peak at 2.4 ppm; this patient did not undergo surgery or a diagnostic biopsy and therefore no tissue was available for further analysis and therefore we have classified this case as borderline.

No succinate peak

No succinate peak was detected in three subjects. Patient #4 had a metastatic wtGIST with no detectable germline *SDHx* mutation and preserved SDHB protein expression in the tumour tissue; choline was confidently fitted on LCModel but no succinate was seen. Patient #6 demonstrated a good quality spectrum from the remnant pituitary adenoma; choline was detected on LCModel and SAGE processing but no succinate was detected and this finding was consistent with the preservation of SDHB protein expression in the pituitary tumour by immunohistochemistry (Figure 4). Patient #10 had no detectable germline *SDHx* mutation and preserved SDHB protein expression in the tumour tissue; choline was detected in the tumour on ^{1}H-MRS but succinate was not detected.

Technical failure

Technical failure occurred in four patients (26%). Patient #12 demonstrated no reliable detection of succinate or choline due to motion artefact and a low signal-to-noise ratio (SNR), which was probably due to inconsistent breathing as the voxel was at the edge of the liver. A small rib metastasis was imaged in patient #13 but only a pure lipid spectrum was obtained from this challenging location. A metastasis on the edge of the liver was imaged in patient #14, where again inconsistent respiration probably led to displacement of the voxel into adjacent adipose tissue. Finally, patient #15 had a unilateral phaeochromocytoma with a large volume of blood, whose paramagnetic properties may have affected acquisition leading to low SNR (Supplementary Table S1).

Sequential ^{1}H-MRS succinate analysis

Subject #2 with a metastatic paraganglioma to the lung, bone and lymph node and a germline *SDHB* mutation *(*c.268C>T p.Arg90*) underwent ^{1}H-MRS on a large pelvic nodal metastasis prior to treatment with four cycles of lutetium 177-labelled peptide receptor radionuclide therapy. Succinate and choline peaks were detected with an SCR of 1.32 (Figures 5a, 5b). Following four cycles of treatment, a repeat ^{1}H-MRS examination on the same pelvic nodal metastases revealed a choline peak but no succinate peak (Figure 5c). Though the MRI imaging features of the metastatic lesions were unchanged pre- and post-treatment, the loss of a succinate peak was correlated with a reduction in plasma normetanephrine levels (from 1861 to 1193 pmol/L) and tumour avidity on ^{18}F-fluorodeoxyglucose Positron Emission Tomography/Computed Tomography (FDG-PET/CT; standard uptake value of 16.1 pre-treatment and 9.3 post-treatment; Figure 5d-f). The detection of choline on the acquired spectra both before and after treatment indicates that tumour necrosis is unlikely to account for the absent succinate peak post treatment.

A sequential ^{1}H-MRS study was performed on patient #5 due to evidence of progressive disease on surveillance CT, despite treatment with a multi-kinase inhibitor, regorafenib. Serial ^{1}H-MRS demonstrated a larger succinate peak compared to the first study (Figure 2d and 2e) and this correlated with the FDG avidity on PET/CT pre-treatment and ten months post-treatment, which demonstrated an increase in disease burden and avidity (SUV: 15.1 and 27.1 respectively, Figures 2f-g).

Repeatability of ^{1}H-MRS was evaluated in two patients by investigating different tumour deposits during the same study examination (case#5) and the same tumour deposit twice during the same study examination (case#1). The results for succinate: choline were almost identical in these two cases, suggesting good test reproducibility (Supplementary Table 2)

Discussion

This proof-of-principle study has demonstrated that detection of a succinate peak and an increased succinate to choline ratio were specific for a variety of SDH-deficient tumour types. All six tumours with a positive succinate peak and elevated SCR were associated with a germline *SDHx* mutation (n = 4) or an *SDHC* epimutation (n = 2). In addition, the three subjects with absent succinate peaks but adequate ^{1}H-MRS, demonstrated preservation of SDHB expression in the tumour analyzed. Our findings are complementary to a previous study in which ^{1}H-MRS was applied to 9 patients with paraganglioma and a succinate peak was detected in all 5 with an *SDHx* mutation but not in the 4 patients without a mutation[16]. We have demonstrated for the first time that ^{1}H-MRS can also be used to determine the SDH status of GISTs and pituitary adenomas and that a succinate peak can be detected in SDH-deficient tumours with epigenetic inactivation of *SDHC*. There are a wide variety of situations in which ^{1}H-MRS might have clinical utility. Potential diagnostic applications of this new approach include: (a) assessing the pathogenicity of patients with a germline SDHx variants of uncertain significance and a potentially SDH-related tumour; (b) investigating possible metastatic lesions e.g. in the liver, in patients with a germline *SDHx* mutation and a primary SDH-deficient tumour; (c) assessing patients with multiple primary tumours to determine if all are SDH-deficient; (d) identifying patients without a detectable germline *SDHx* mutation who might benefit from specialist genetic investigations such as SDHC promoter methylation status; and (e) assessing SDH tumour status pre-operatively particularly for patients with possible wtGIST as standard adjuvant treatment with imatinib has proven to be less effective in patients with SDH-deficient disease[12].

Notably, here we have used the presence of a choline signal as an internal control for viable tissue to discriminate technical failures from a negative finding. To avoid issues of partial voluming effects within smaller tumours, the voxel for MRS analysis was chosen to fully

include tumour where possible. We did not detect a statistically significant correlation between tumour size and succinate/choline ratio although there was a trend towards significance. This trend is the opposite of what would be expected if necrosis was artificially lowering the overall succinate levels in large tumours, and therefore suggests that the method is measuring real differences in succinate, which are independent of tumour size. However, we recommend using a size threshold of greater than 2 cm where possible to improve the sensitivity of the test.

There is increasing interest in understanding the metabolic adaptations that occur during tumorigenesis and how these might be exploited for novel therapeutic interventions. Increased production of lactate during aerobic glycolysis in most cancers, or the Warburg effect, is the best known example of this. SDH-related cancers provides a paradigm for investigating tumour metabolism as succinate is thought to act as an oncometabolite and to drive tumorigenesis[6]. Succinate inhibits 2-oxoglutarate-dependent dioxygenases including DNA and histone demethylases and hypoxic gene response regulators. As a consequence, SDH-deficient tumours demonstrate epigenetic abnormalities, an activated hypoxic gene response and more recently there is evidence that succinate may have a paracrine effect on stromal tissue[20, 21, 22]. Understanding the molecular mechanisms of SDH-related tumorigenesis provides a rationale for novel therapeutic interventions such as reversing the epigenetic abnormalities or exploiting metabolic vulnerabilities, similar to the recent discovery that tumoral 2-hydroxyglutarate accumulation may increase responsiveness to olaparib, a poly-ADP-ribose polymerase (PARP) inhibitor[23]. The availability of sensitive non-invasive biomarkers would greatly facilitate precision medicine-based clinical trials. Imaging with ^{18}F-FDG PET to measure the uptake and phosphorylation of a glucose-analogue to probe the increased glucose utilisation that occurs in many metabolically-active cancers, is a useful form of *in vivo* metabolic imaging and has been employed for the

detection of primary and metastatic disease in many tumour types including PPGL and GIST[24, 25] and is in widespread clinical use. However, despite being a very sensitive imaging tool, ^{18}F-FDG PET lacks specificity and cannot differentiate individual metabolites. ^{1}H-MRS is highly specific and allows *in vivo* detection of individual metabolites without the use of ionising radiation, however, ^{1}H-MRS is significantly less sensitive than PET, which could limit the detection of low levels of succinate and it can be challenging to differentiate intracellular from extracellular metabolites. In the future, ^{1}H-MRS may be complemented by other techniques such as hyperpolarised ^{13}C-MR spectroscopic imaging, which can increase MR signal-to-noise by several orders of magnitude allowing assessment of enzyme flux *in vivo*[26].

We have shown that ^{1}H-MRS could be a valuable tool for the assessment of tumour response in the context of radionuclide and other therapies as alterations in succinate levels were detected despite stable appearances of the tumour diameter. This important application of ^{1}H-MRS could be expanded to include other tumours with specific metabolic defects including fumarate hydratase deficient tumours[27], *IDH1* mutant tumours[28] and the recently identified malate dehydrogenase 2 (MDH2) deficient tumours[29]. However, important limitations of *in vivo* metabolomic analysis using ^{1}H-MRS were also revealed by our study: for example, spectral quality was poor in close proximity to metal dental work, adjacent to air spaces including the lung, in bone metastases, and was susceptible to motion artefact. In this study, the technical failure rate was 26%, which is similar to the failure rate reported in previous studies using ^{1}H-MRS[16]. Importantly, no cases was excluded from this prospective study, with the intention that this would inform on the translation of this imaging modality into clinical practice. Based on the evidence from this exploratory study, we would recommend that tumours were selected for ^{1}H-MRS analysis based on: (i) ideally the largest tumour

deposit but at least a size greater than 2 cm, (ii) tumours located close to bone or lung should be avoided, (iii) tumours with significant necrosis or hemorrhage should be avoided, (iv) superficial tumour deposits should be selected preferentially, and (v) respiratory triggered acquisition should be used for tumours in the upper abdomen, such as hepatic metastases. Although the use of ^{1}H-MRS as a diagnostic tool is likely to be limited to specialist centres, the number of scan averages in our study during spectral acquisition was less than half those reported in a previous study[16] (200 versus 512), without demonstrating a reduction in sensitivity. Using fewer scan averages reduces the acquisition time, making it more cost effective and convenient for the patient. This is a particularly important consideration if this imaging technique is to be considered for routine clinical practice or for sequential follow-up as part of a clinical trial. Furthermore this imaging modality could be used to investigate other metabolically-driven tumours.

In conclusion, this study is the largest to date to evaluate ^{1}H-MRS in patients with SDH deficiency. It has revealed that ^{1}H-MRS has the potential to be used as a non-invasive biomarker in the precision management of SDH-deficient disease and could have a role as a biomarker of successful treatment response. Lessons learned from this study could be applied to other similar metabolically-driven tumours.

353 **References**

354 1. Astuti D, Latif F, Dallol A, et al. Gene mutations in the succinate dehydrogenase subunit
355 SDHB cause susceptibility to familial pheochromocytoma and to familial paraganglioma. Am
356 J Hum Genet 2001;69:49–54.

357 2. Baysal BE, Ferrell RE, Willett-Brozick JE, et al. Mutations in SDHD, a mitochondrial
358 complex II gene, in hereditary paraganglioma. Science. 2000 Feb 4;287(5454):848-51.

359 3. K.A. Janeway, S.Y. Kim, M. Lodish, et al. Defects in succinate dehydrogenase in
360 gastrointestinal stromal tumors lacking KIT and PDGFRA mutations. Proc. Natl. Acad. Sci.
361 USA 2011;108, 314–318.

362 4. Vanharanta S, Buchta M, McWhinney SR, et al. Early-onset renal cell carcinoma as a
363 novel extraparaganglial component of SDHB-associated heritable paraganglioma. Am J Hum
364 Genet 2004;74:153–159.

365 5. Xekouki P, Stratakis CA. Succinate dehydrogenase (SDHx) mutations in pituitary tumors:
366 could this be a new role for mitochondrial complex II and/or Krebs cycle defects? Endocr
367 Relat Cancer 2012;19:C33–C40.

368 6. Cecchini, G. Respiratory complex II: Role in cellular physiology and disease. Biochim.
369 Biophys. Acta (BBA)-Bioenerg. 1827, 541–542 (2013).

370 7. Morin A, Letouzé E, Gimenez-Roqueplo AP, et al. Oncometabolites-driven tumorigenesis:
371 From genetics to targeted therapy. Int J Cancer. 2014 Nov 15;135(10):2237-48. doi:
372 10.1002/ijc.29080.

373 8. Pritchett JW. Familial occurrence of carotid body tumor and pheochromocytoma. Cancer
374 1982 49 2578–2579.

9. Gimenez-Roqueplo AP, Favier J, Rustin P, et al. COMETE Network. Mutations in the SDHB gene are associated with extra-adrenal and/or malignant phaeochromocytomas. Cancer Res. 2003;63:5615–5621.

10. Evenepoel L, Papathomas TG, Krol N, et al. Toward an improved definition of the genetic and tumor spectrum associated with SDH germ-line mutations. Genet Med. 2015 Aug;17(8):610-20. doi: 10.1038/gim.2014.162.

11. Boikos SA, Pappo AS, Killian JK, et al. Molecular Subtypes of KIT/PDGFRA Wild-Type Gastrointestinal Stromal Tumors: A Report from the National Institutes of Health Gastrointestinal Stromal Tumor Clinic. JAMA Oncol. 2016 Jul 1;2(7):922-8. doi: 10.1001/jamaoncol.2016.0256.

12. Mason EF, Hornick JL. Conventional Risk Stratification Fails to Predict Progression of Succinate Dehydrogenase-deficient Gastrointestinal Stromal Tumors: A Clinicopathologic Study of 76 Cases. Am J Surg Pathol. 2016 Jun 23.

13. Ricketts C, Woodward ER, Killick P, et al. Germline SDHB mutations and familial renal cell carcinoma. J Natl Cancer Inst. 2008 Sep 3;100(17):1260-2. doi: 10.1093/jnci/djn254.

14. Amar L, Fassnacht M, Gimenez-Roqueplo AP, et al. Long-term postoperative follow-up in patients with apparently benign pheochromocytoma and paraganglio ma. Hormone and Metabolic Research 2012 44 385–389.

15. Richter S, Peitzsch M, Rapizzi E, et al. Krebs cycle metabolite profiling for identification and stratification of pheochromocytomas/paragangliomas due to succinate dehydrogenase deficiency. J Clin Endocrinol Metab 2014;99:3903–11.

16. Varoquaux A, le Fur Y, Imperiale A, et al. Magnetic resonance spectroscopy of paragangliomas: new insights into in vivo metabolomics. Endocr Relat Cancer. 2015 Aug;22(4):M1-8. doi: 10.1530/ERC-15-0246. Epub 2015 Jun 26.

17. Lussey-Lepoutre C, Bellucci A, Morin A, et al. In Vivo Detection of Succinate by Magnetic Resonance Spectroscopy as a Hallmark of SDHx Mutations in Paraganglioma. Clin Cancer Res. 2016 Mar 1;22(5):1120-9. doi: 10.1158/1078-0432.CCR-15-1576. Epub 2015 Oct 21.

18. Andronesi OC, Rapalino O, Gerstner E, at al. Detection of oncogenic IDH1 mutations using magnetic resonance spectroscopy of 2-hydroxyglutarate. J Clin Invest. 2013 Sep;123(9):3659-63. doi: 10.1172/JCI67229.

19. Provencher SW. Estimation of metabolite concentrations from localized in vivo proton NMR spectra. Magn Reson Med. 1993 Dec;30(6):672-9.

20. Xu, W, Yang, H., Liu, Y., et al. (2011). Oncometabolite 2-hydroxyglutarate is a competitive inhibitor of a-ketoglutarate-dependent dioxygenases. Cancer Cell 19,17–30.

21 Letouze, E , Martinelli C, Loriot C, et al. SDH mutations establish a hypermethylator phenotype in paraganglioma. Cancer Cell 23, 739–752 (2013).

22. Garrigue P, Bodin-Hullin A, Balasse L, et al. The evolving role of succinate in tumor metabolism: an ^{18}F-FDG-based study. J Nucl Med. 2017 Jun 15. pii: jnumed.117.192674. doi: 10.2967/jnumed.117.192674.

23. Sulkowski PL, Corso CD, Robinson ND, et al. 2-Hydroxyglutarate produced by neomorphic IDH mutations suppresses homologous recombination and induces PARP inhibitor sensitivity. Sci Transl Med. 2017 Feb 1;9(375). pii: eaal2463. doi: 10.1126/scitranslmed.aal2463.

419 24. Chang CA, Pattison DA, Tothill RW, et al. ^{68}Ga-DOTATATE and ^{18}F-FDG PET/CT in
420 Paraganglioma and Pheochromocytoma: utility, patterns and heterogeneity.Cancer Imaging.
421 2016 Aug 17;16(1):22. doi: 10.1186/s40644-016-0084-2.

422 25. Holdsworth CH, Badawi RD, Manola JB, et al. CT and PET: early prognostic indicators
423 of response to imatinib mesylate in patients with gastrointestinal stromal tumor. AJR Am J
424 Roentgenol 2007;189:W324-30.

425 26. Day SE, Kettunen MI, Gallagher FA, et al. Detecting tumor response to treatment using
426 hyperpolarized 13C magnetic resonance imaging and spectroscopy. Nat Med. 2007
427 Nov;13(11):1382-7. Epub 2007 Oct 28. Erratum in: Nat Med. 2007 Dec;13(12):1521.

428 27. Clark GR, Sciacovelli M, Gaude E, et al. Germline FH mutations presenting with
429 pheochromocytoma. J Clin Endocrinol Metab. 2014 Oct;99(10):E2046-50.

430 28. Andronesi OC, Rapalino O, Gerstner E, et al. Detection of oncogenic IDH1 mutations
431 using magnetic resonance spectroscopy of 2-hydroxyglutarate. J Clin Invest. 2013
432 Sep;123(9):3659-63. doi: 10.1172/JCI67229.

433 29. Cascón A, Comino-Méndez I, Currás-Freixes M, et al. Whole-exome sequencing
434 identifies MDH2 as a new familial paraganglioma gene. J Natl Cancer Inst. 2015 Mar
435 11;107(5). pii: djv053. doi: 10.1093/jnci/djv053.

436 30. Madhu B, Shaw GL, Warren AY, et al. Response of Degarelix treatment in human
437 prostate cancer monitored by HR-MAS 1H NMR spectroscopy. Metabolomics. 2016;12:120

438 31. Andreasson A, Kiss NB, Caramuta S, et al. The VHL gene is epigenetically inactivated in
439 pheochromocytomas and abdominal paragangliomas. Epigenetics. 2013 Dec;8(12):1347-54.
440 doi: 10.4161/epi.26686. Epub 2013 Oct 22.

441

Funding:

We thank the following funding organisations; GIST Support UK (RC), Cambridge Experimental Cancer Medicine Centre, Addenbrooke's Charitable Trust, National Institute for Health Research (NIHR) Cambridge Biomedical Research Centre, Cancer Research UK CRUK (FAG, MM), CRUK Cambridge Centre (MM, FAG, ERM), the University of Cambridge, and Hutchison Whampoa Ltd (MM), NIHR Senior Investigator Award (ERM), European Research Council Advanced Researcher Award (ERM), the British Heart Foundation (ERM), CRUK and Engineering and Physical Sciences Research Council (EPSRC) Imaging Centre in Cambridge and Manchester (FAG). The University of Cambridge has received salary support in respect of EM from the NHS in the East of England through the Clinical Academic Reserve.

Acknowledgements:

The authors would like to thank Stephen Provencher for providing the simulated basis set used in spectral fitting, the radiographers and staff of the MRIS Unit at Addenbrooke's Hospital and the staff of the Tissue Bank at Addenbroke's hospital for assistance, and all the patients who participated in this study.

464 **Tables:**

465 **Table 1:** Clinical characteristics of the cohort. PA = pituitary adenoma, PC =
466 phaeochromocytoma.

Case number	**Genetic mutation**	**Sex**	**Age**	**Primary tumour**	**Metastatic disease**	**Site of metastatic disease**	**Family history**	**Other primary tumour**
1	*SDHC* epimutation	F	21	GIST	Yes	Liver, lung	No	No
2	*SDHB* c.268C>T p.(Arg90*)	F	53	Abdominal PGL	Yes	Lymph nodes, bone	Yes-mother (GIST)	No
3	*SDHC* epimutation	F	25	GIST	Yes	Liver	No	No
4	No mutation detected	F	27	GIST	No	NA	No	No
5	*SDHB* c.137G>A p.(Arg46Gln)	M	38	GIST	Yes	Liver, peritoneum	No	No
6	*SDHB* c.380G>T p.(Ille127Ser)	M	80	PA	No	NA	Yes nephew (PPGL)	No
7	No mutation detected	M	70	PC	Yes	Liver, bone	No	No

8	*SDHB* c.600G>T p.(Trp200Cys)	M	41	Glomus PGL	No	NA	No	Yes, PA
9.	*SDHB* c.302G>A p.(Cys101Tyr)	M	26	Abdominal PGL	No	NA	No	Carotid PGL
10.	No mutation detected	M	23	PC	No	NA	No	No
11.	*SDHA* c.91C>T p.(Arg31Ter)	F	21	GIST	Yes	Liver	No	No
12.	*SDHA* c.1765C>T p.(Arg589Trp)	F	37	GIST	Yes	Liver	No	No
13	*SDHA* *c.91C>T* *p.(Arg31Ter)*	M	46	PGL	Yes	Bone	No	No
14	*SDHA* *c.91C>T* *p.(Arg31Ter)*	M	24	GIST	Yes	Liver	No	No
15	No mutation	M	67	PC	No	NA	No	No

467

468 **Figure legends**

469 Figure 1. (A): T_2-weighted MR image from case 1 and (B) T_1-weighted image from case 3
470 demonstrating liver metastases from which spectra were acquired in the locations indicated

by the white arrows. (C-D) show the spectra from case 1 and case 3 demonstrating a succinate peak at 2.4 ppm. (E-F) demonstrate hypermethylation of the promoter region of the SDHC gene in tumour DNA from cases 1 and 3, confirming a somatic SDHC epimutation: 55% mean methylation in case 1 and 75% mean methylation in case 3.

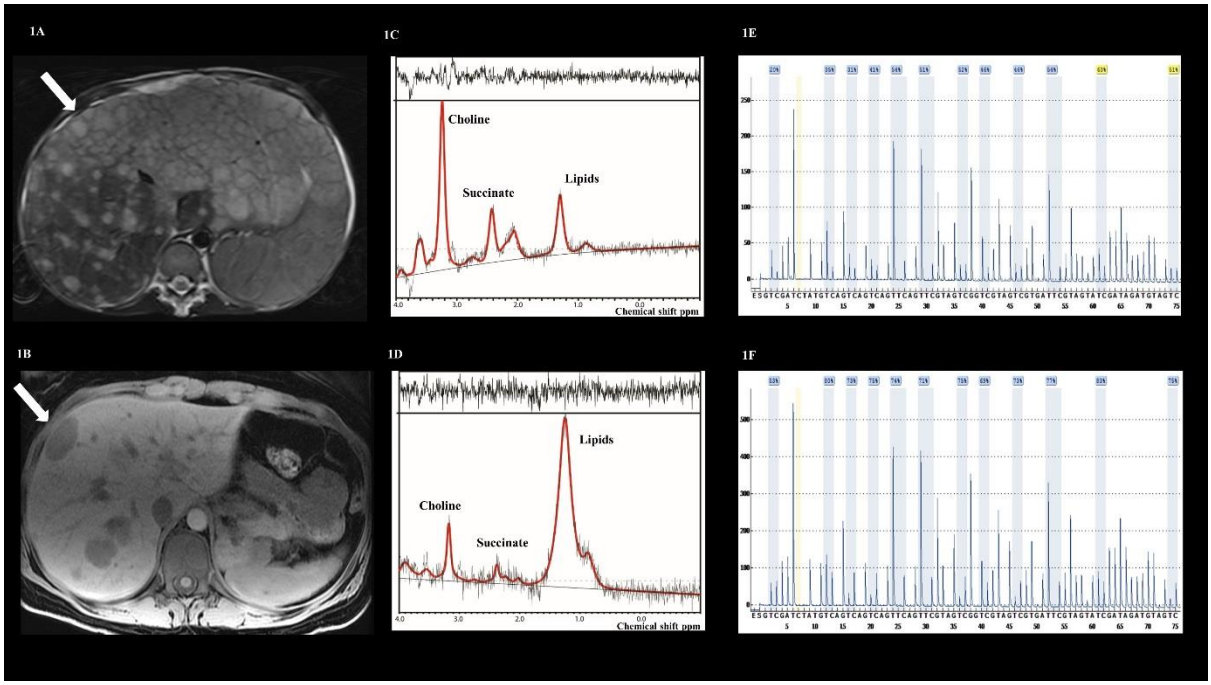

Figure 2. (A) T_1-weighted MR image of a metastatic GIST to the liver (arrow) from case 5. (B) SDHB immunonegativity on SDHB immunohistochemistry performed on the wt GIST tumour from the same patient. (C) Axial fused ^{18}F-FDG PET/CT image demonstrating an FDG-avid carotid body PGL after SDH deficiency was demonstrated on ^{1}H-MRS. (D-E) Spectra acquired at ^{1}H-MRS from the same case before and during treatment with a multi-kinase inhibitor. (F-G) Axial fused ^{18}F-FDG PET/CT images and corresponding coronal PET projections illustrating the increase in disease burden and FDG avidity over time (SUV: 15.1 and 27.1) which correlates with the increase in the succinate peak demonstrated on ^{1}H-MRS.

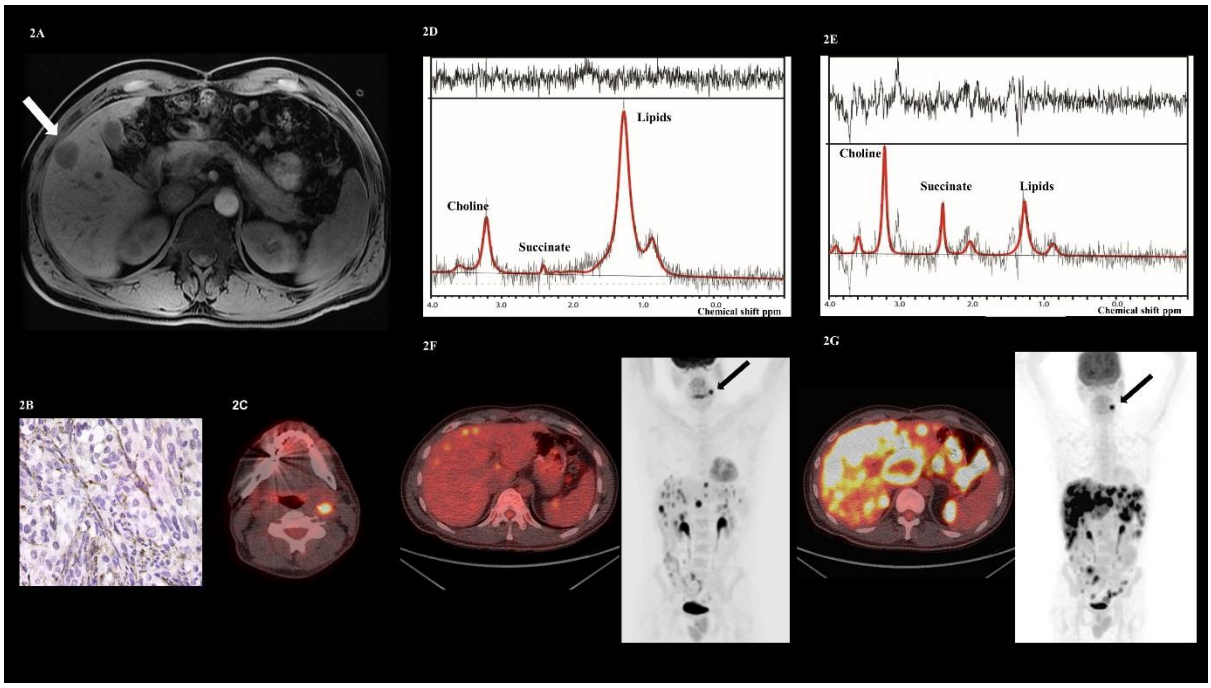

Figure 3. (A) T_2-weighted MRI showing a large non-secretory abdominal paraganglioma from case 9 (arrow). (B) ^{1}H-MR spectra demonstrating a succinate peak at 2.4 ppm. (C) Axial fused ^{18}F-FDG PET/CT image. The corresponding coronal maximum intensity projection (MIP) PET image demonstrates a synchronous left sided carotid paraganglioma. (D) Spectra acquired by High Resolution Magic Angle Spinning (HR-MAS) *in vitro* on the paraganglioma tumour sample, again confirming a succinate peak at 2.4 ppm.

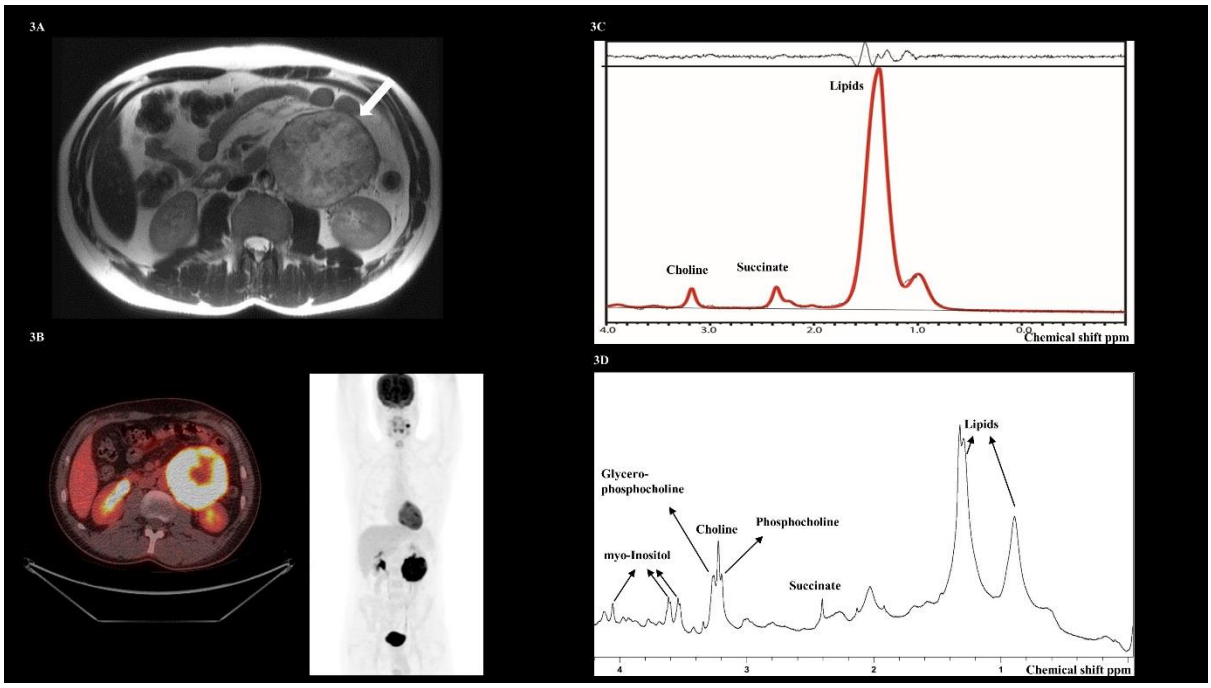

493

494

495 **Figure 4:** (A) Coronal T_1-weighted MRI demonstrating a remnant pituitary adenoma in case
496 6 (white arrow). (B) Spectra acquired from the pituitary tumour at ^{1}H-MRS, with evidence of
497 choline detection but no succinate. (C) SDHB IHC demonstrating preservation of the SDHB
498 protein performed on a section of tumour tissue debulked from the pituitary tumour.

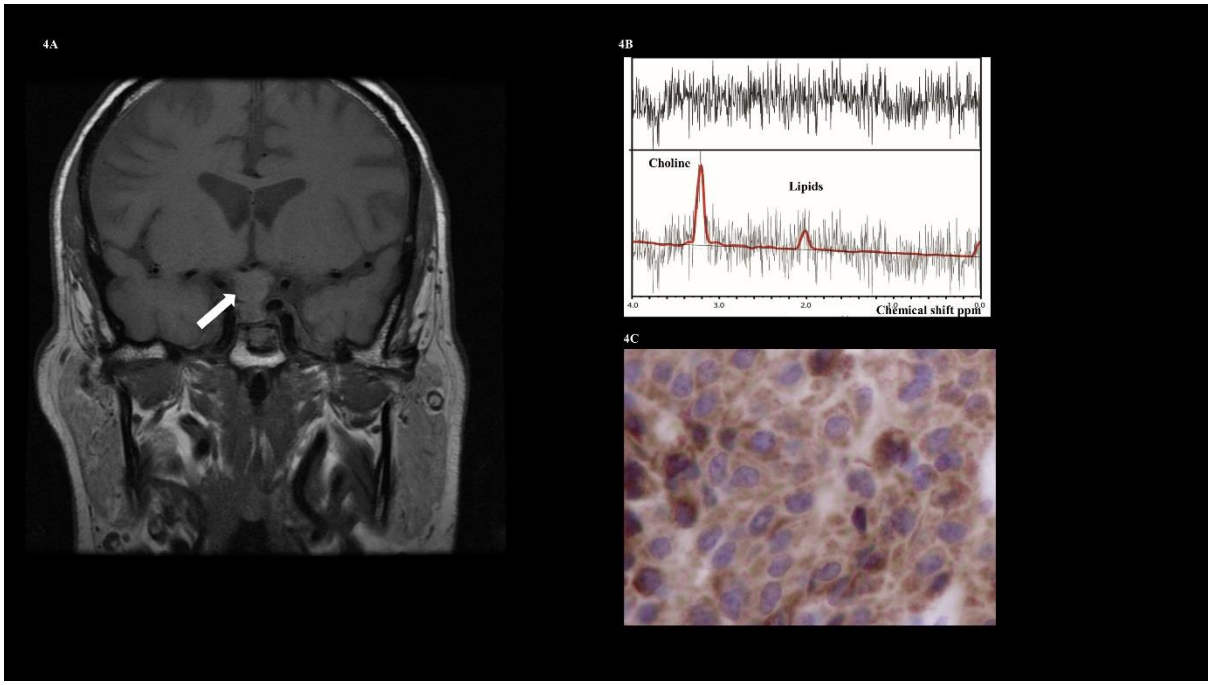

499

Figure 5. (A) Axial T_2-weighted MRI image of a retroperitoneal nodal metastases from case 2 (arrow). (B) Spectra acquired before treatment illustrating succinate accumulation at 2.4 ppm. (C) Spectra acquired following 4 cycles of [^{177}Lu]-DOTATATE with no detectable succinate peak at 2.4 ppm. (D) Plasma metanephrine and methoxytyramine levels before and after treatment with [^{177}Lu]-DOTATATE. (E) Axial fused ^{18}F-FDG PET/CT image and corresponding coronal PET projection showing the FDG-avid nodal metastases (SUV = 16.1, arrowed). (F) The same nodal metastases following treatment with [^{177}Lu]-DOTATATE demonstrating reduced tracer uptake in keeping with the biochemical findings (SUV = 9.3).

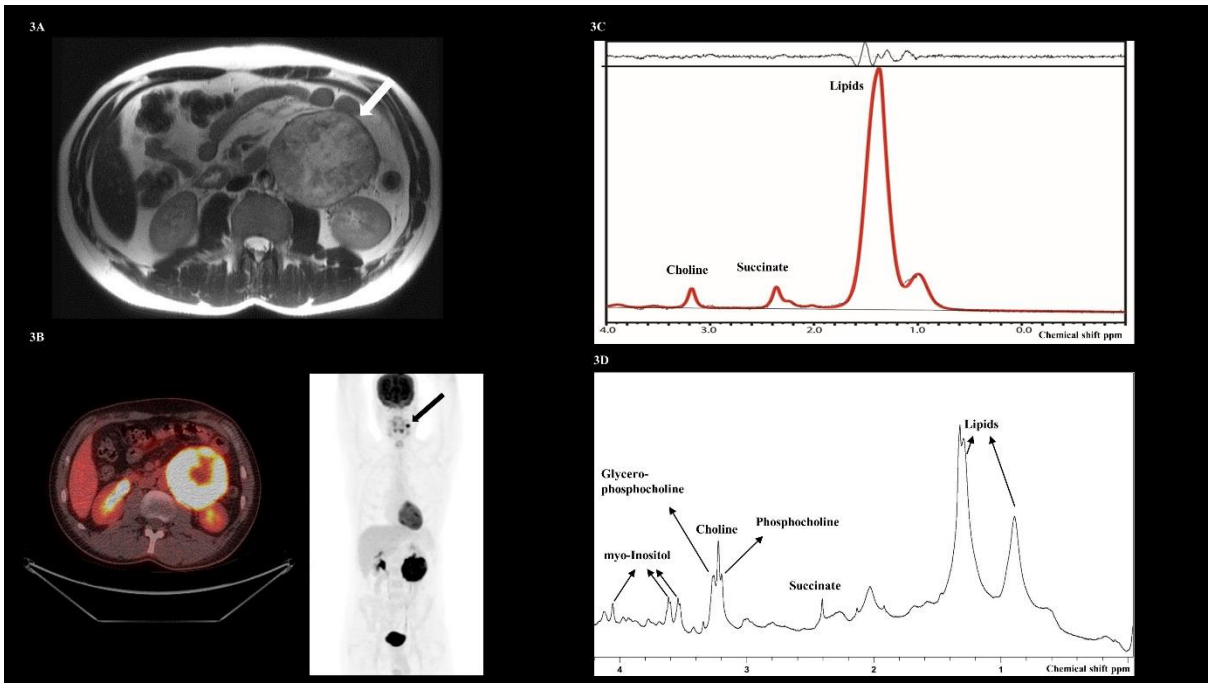

Supplementary data:

Figure S1: (A) Coronal MRI image of a large left sided glomus paraganglioma from case 8 demonstrated by the white arrow. (B) Spectra processed with LCModel from the same patient showing a broad unreliable peak at 2.4 ppm, which was not convincing for succinate.

Table S1: Characteristics of the 15 tumours analysed by ^{1}H-MRS. TF: technical failure, defined as an estimated uncertainty (%SD) > 15% in automated peak fitting of choline using LCModel. ND: not detected. NA: not applicable.

Table S2: Characteristics of the two patients in whom ^{1}H-MRS was repeated during the same examination to evaluate test reproducibility.